Dynamics of the F_2 Reaction with Propene: The Effect of Methyl Substitution†

Jing-Wen Fang,[‡,§] Tingxian Xie,[‡,||] Hsueh-Ying Chen,[‡] Yu-Ju Lu,[‡] Yuan T. Lee,[‡,§] and Jim J. Lin*[,‡,⊥]

Institute of Atomic and Molecular Sciences, Academia Sinica, Taipei 10617, Taiwan, Department of Chemistry, National Taiwan University, Taipei 10617, Taiwan, Department of Physics, Dalian Jiaotong University, Dalian, Liaoning 116028, China, and Department of Applied Chemistry, National Chiao Tung University, Hsinchu 30010, Taiwan

Received: December 15, 2008; Revised Manuscript Received: January 9, 2009

The reaction of $F_2 + C_3H_6$ has been investigated with the crossed molecular beam technique. The only observed primary product channel is $F + C_3H_6F$ while the $HF + C_3H_5F$ channel cannot be found. The reaction cross section was measured as a function of collision energy and the reaction threshold was determined to be 2.4 ± 0.3 kcal/mol. Compared to the reaction threshold of the $F_2 + C_2H_4$ reaction, the methyl substitution effectively reduces the reaction threshold by about 3 kcal/mol. The product time-of-flight spectra and angular distributions were measured and analyzed. The angular distribution displays strongly backward, indicating that the reaction is much faster than rotation. All experimental results support a rebound reaction mechanism, which agrees with the structure of the calculated transition state. The transition state geometry also suggests an early barrier; such dynamics is consistent with the observed small kinetic energy release of the products. Except for the different values of the reaction thresholds, the dynamics of the $F_2 + C_2H_4$ and $F_2 + C_3H_6$ reactions are remarkably similar.

Introduction

The fluorination of olefin molecules is important in organic chemistry.[1] In 1956, Miller and co-workers suggested that the reaction of molecular fluorine with olefin proceeded via an initiation step with productions of a fluorine atom and a free fluoro radical.[2−4] However, the reaction mechanism was not universally accepted due to the lack of further experimental evidence. Our previous study[5] on the reaction of molecular fluorine with ethylene has provided clear experimental and theoretical evidence to verify the suggestion of Miller et al. The investigations on the $F_2 + C_2H_4$ reaction with crossed molecular beam experiments and high-level ab initio calculations indicate that the primary product channel is $F + C_2H_4F$. But under matrix isolation conditions, $C_2H_4F_2$ and $HF + C_2H_3F$ were observed to be the products of the same reaction.[6−10] After carefully considering all possibilities, we found the most reasonable explanation for the totally different products observed in the condensed phase is due to the steric cage effect and secondary reactions which are absent in the gas phase conditions.[5,11−14]

In this work, we extend the investigation to the reaction of molecular fluorine with methyl-substituted ethylene, C_3H_6. The initial motivation was to search for a direct HF formation channel in the F_2 reactions with olefins. The idea is based on the molecular geometries. After the F_2 attack on the π-bond of ethylene, we thought, the four H atoms on the C_2H_4 are all quite far away from the F atoms, such that the probability of HF formation would be very small. This probability may be enhanced for a methyl-substituted ethylene, which is a nonplanar molecule, and the H atoms on the methyl group may have a chance to be closer to the F atoms. Whether the HF channel exists in the $F_2 + C_3H_6$ reaction may provide important mechanistic information regarding the fluorination of olefins.

Hauge et al.[6] have investigated the reactivity of molecular fluorine with small hydrocarbons including $F_2 + C_3H_6$. These reactions were studied in pure fluorine or argon−fluorine matrices at 15 K. They reported that the propylene, butadiene, and cyclohexene reacted with F_2 spontaneously even at such a low temperature, but the occurrence of a reaction for ethylene and allene required additional exposure to near-infrared photons of 1 to 4 μm wavelength. In addition, neither the alkanes nor alkynes could react with F_2 at 15 K even after exposure to the near-infrared radiation for a long time. The reactivity of benzene also was found to be small. Their results suggest that the activation energies of these fluorination reactions may be in the order of:

$$\text{propylene} \approx \text{butadiene} \approx \text{cyclohexene} < \text{ethylene} \approx \text{allene} < \text{benzene, alkane, alkyne.}$$

This discovery gave rise to another motivation. The result of Hauge et al.[6] strongly suggests that the methyl substitutions in small alkenes substantially reduce the activation energies of the F_2 reactions. Moreover, the experimental threshold of the $F_2 + C_2H_4$ reaction has been measured to be 5.5±0.5 kcal/mol with the crossed molecular beam technique.[5] However, the high-level ab initio calculation gives a value of 7.08 kcal/mol for the reaction barrier.[5] Although the discrepancy of about 1.6 kcal/mol between the experimental and theoretical reaction barriers is still within a reasonable error bar of the CCSD(T) level of theory,[15,16] it is meaningful to ask whether this discrepancy is systematic in similar reaction systems. The $F_2 + C_3H_6$ reaction may offer a good opportunity to test the errors of reaction barriers for the CCSD(T) method, which has been widely used in chemical kinetics calculations.

† Part of the "George C. Schatz Festschrift".
* Address correspondence to this author.
‡ Academia Sinica.
§ National Taiwan University.
|| Dalian Jiaotong University.
⊥ National Chiao Tung University.

10.1021/jp811053d CCC: $40.75
Published on Web 02/11/2009

Methods

The experimental apparatus has been described.[17] The C_3H_6 gas (99.5%, Matheson) was seeded (10−30%) in He or Ne and expanded through a fast pulsed valve[18] to form a supersonic molecular beam. The F_2 molecular beam was generated by expanding either 10% F_2 in Ne or neat F_2 gas through a similar pulsed valve that could be cooled to −120 °C. Depending on the gas mixing ratios and nozzle temperatures, the mean speed of the F_2 beam was tuned from 530 to 795 m/s and the mean speed of the C_3H_6 beam was tuned from 780 to 1360 m/s to have various collision energies. The rest of experimental procedures and data analysis are similar to the previous work on $F_2 + C_2H_4$.[5]

High-level ab initio calculations including using the CASPT2, CCSD(T), and B3LYP methods in various regions on the potential energy surface of the $F_2 + C_3H_6$ reaction were performed with the MOLPRO2006.1 quantum chemistry package.[19] The selection of basis sets and detailed calculation procedures are also similar to those mentioned in ref 5.

Results

A. Identification of Product Channels. Possible products were carefully searched for in the $F_2 + C_3H_6$ reaction. For convenience of the following discussions, four possible channels can be listed as:

$$F_2 + C_3H_6 \rightarrow C_3H_6F_2 \quad \text{(R1)}$$

$$F_2 + C_3H_6 \rightarrow C_3H_6F + F \quad \text{(R2)}$$

$$F_2 + C_3H_6 \rightarrow C_3H_5F + HF \quad \text{(R3)}$$

$$F_2 + C_3H_6 \rightarrow C_2H_3F + CH_3F \quad \text{(R4)}$$

Although the formation of reaction R1 is not likely because the reaction exothermicity of reaction R1 exceeds the dissociation barrier of $C_3H_6F_2$, we have searched for signals at mass-to-charge ratios (m/z) of 80 ($C_3H_6F_2^+$), 79 ($C_3H_5F_2^+$), and 65 ($C_2H_3F_2^+$) at the center-of-mass angle. No signal can be observed as one may expect.

The F atom formation channel has been observed in the $F_2 + C_2H_4$ reaction. For the methyl-substituted analogue, the product of reaction R2 can be measured at the masses of the parent ion (m/z 61) of C_3H_6F and its daughter ions, including $C_3H_5F^+$ (m/z 60), $C_3H_4F^+$ (m/z 59), $C_3H_3F^+$ (m/z 58), $C_3H_2F^+$ (m/z 57), C_3HF^+ (m/z 56), $C_2H_5F^+$ (m/z 48), $C_2H_4F^+$ (m/z 47), $C_2H_3F^+$ (m/z 46), $C_2H_2F^+$ (m/z 45), and CH_2F^+ (m/z 33). The assignment of these daughter ions is based on the observation that they possess almost identical time-of-flight (TOF) spectra and angular distributions as the parent ion. Figure 1 shows an example for m/z 61, 60, and 46. The most intense signal observed is at m/z 46. To lose a methyl group during the electron impact ionization process is quite likely for many hydrocarbon molecules, including the reaction R2 product C_3H_6F. In addition, the angular distribution of the hypothetical reaction R1 product would be very narrow because of zero recoil velocity, but this signal has not been observed at the above mentioned masses.

For the HF formation channel R3, its coproduct would show up at the parent ion (m/z 60) and daughter ions of C_3H_5F. However, because reaction R3 is quite exothermic and produces two closed-shell molecules, the translational energy release of the reaction R3 products should be large. If there is any C_3H_5F product from reaction R3, its arrival time will be much shorter than the C_3H_6F product of reaction R2. The absence of any signal before 200 μs in Figure 1 indicates this possibility is little. A similar argument can be applied to reaction R4 which also produces two closed-shell products. Again, all observed signals cannot be assigned to reaction R4.

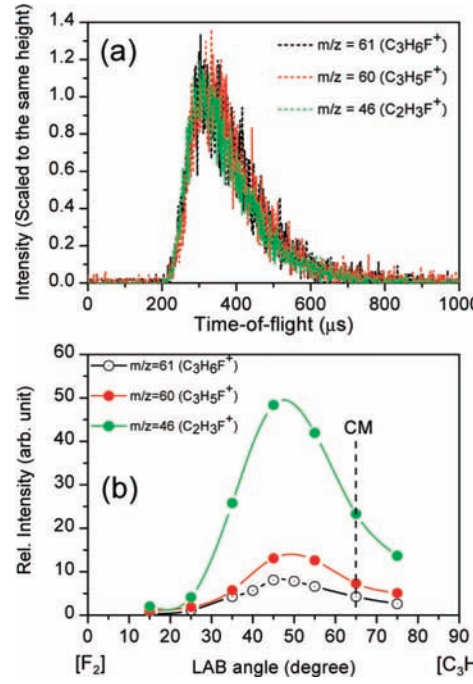

Figure 1. (a) Typical time-of-flight (TOF) spectra of the parent ion of the C_3H_6F product (m/z 61) and its daughter ions, m/z 60 ($C_3H_5F^+$) and 46 ($C_2H_3F^+$), recorded at $\theta_{LAB} = 45°$. (b) Laboratory (LAB) frame angular distributions of signals at m/z 61, 60, and 46. The collision energy is 5.6 kcal/mol. The corresponding LAB angle of the center of mass is indicated as a vertical dashed line.

Although one of the motivations is to search for the HF formation channel, the failure to observe the C_3H_5F coproduct indicates that the HF formation channel either does not exist or is very minor. Still, the F atom + fluoro-radical channel (reaction R2) is the only product channel that can be observed in the $F_2 + C_3H_6$ reaction, analogous to the $F_2 + C_2H_4$ reaction.

B. Product Distributions. Figures 2 and 3 show the experimental TOF spectra of the C_3H_6F product (reaction R2) from the $F_2 + C_3H_6$ crossed beam reaction at collision energies of 3.5 and 5.0 kcal/mol, respectively. The m/z 46, a daughter ion of the C_3H_6F product, was chosen because of higher signal-to-noise ratio and the smallest impurity interference from both molecular beams. We have checked this type of interference by replacing one of the reactant beams with a non-reactive one of a similar mass and velocity. For example, a 10% Ar/Ne beam was used to replace the 10% F_2/Ne beam to check the impurity contribution from the C_3H_6 molecule beam. We have confirmed that the impurity contribution is negligible in the coverage of our detection angles.

To comprehend the reaction dynamics, the laboratory (LAB) frame TOF spectra and angular distributions were transformed to the center-of-mass (CM) frame by using a forward convolution method.[20] The CM frame $P(E_T)$ and $P(\theta_{CM})$ were iteratively adjusted until they fit the experimental data. The best-fit results in the CM frame are plotted in Figure 4. In the beginning, one set of $P(E_T)$ and $P(\theta_{CM})$ was assumed to describe the experimental data, but this assumption cannot fit the entire data satisfactorily. Therefore two channels were used to simulate the whole experimental data. The total reactive flux $P(E_T, \theta_{CM})$ can be represented as:

$$P(E_T, \theta_{CM}) = c_1 P_1(E_T) P_1(\theta_{CM}) + c_2 P_2(E_T) P_2(\theta_{CM})$$

The values of c_1 and c_2 are the weightings of ch1 and ch2, respectively. The weighting of ch2 is only 2% at both collision

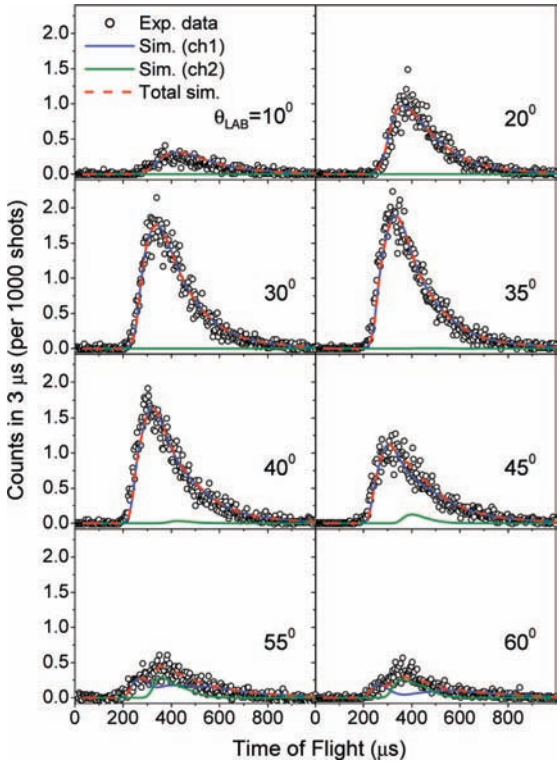

Figure 2. TOF spectra of the C_3H_6F product from the F_2 + C_3H_6 reaction at 3.5 kcal/mol collision energy. Two channels shown as blue and green lines are used to simulate the experimental data. The speeds of the molecular beams are 688 m/s for F_2 and 956 m/s for C_3H_6; the corresponding LAB angle of the center of mass is about 57°. Here the θ_{LAB} indicates the angle in the LAB frame with respect to the F_2 beam direction.

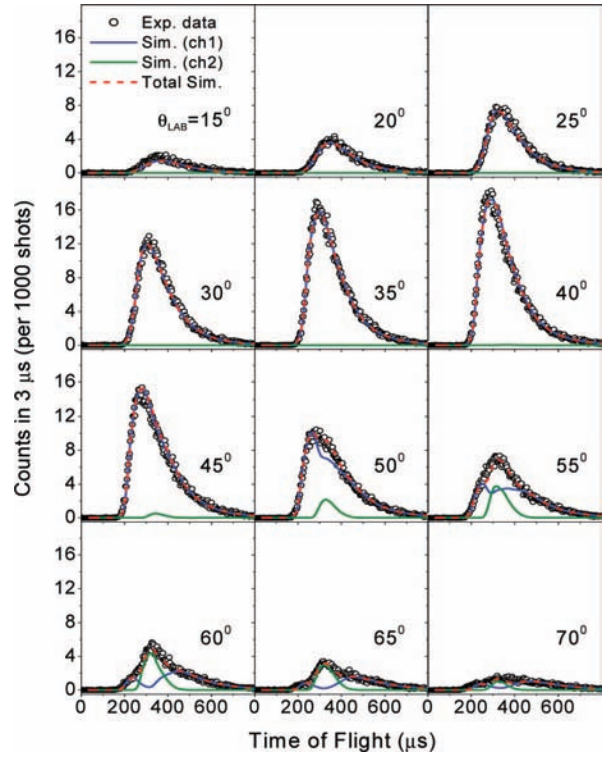

Figure 3. TOF spectra of the C_3H_6F product from the F_2 + C_3H_6 reaction at 5.0 kcal/mol collision energy. The speeds of the molecular beams are 795 m/s for F_2 and 1175 m/s for C_3H_6; the corresponding LAB angle of the center of mass is about 59°.

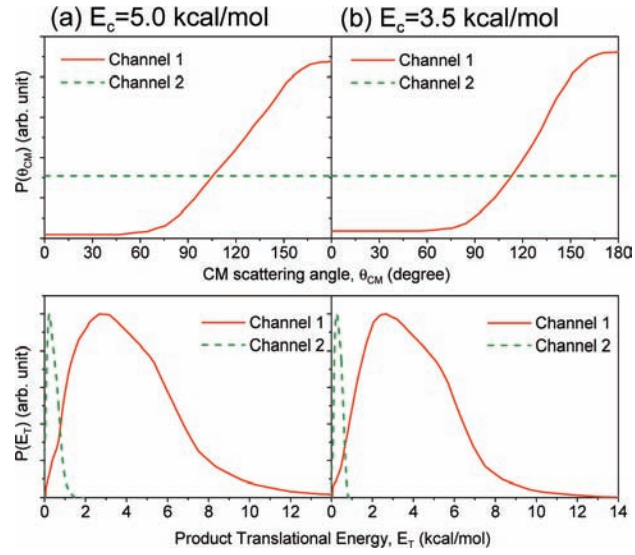

Figure 4. CM-frame translational energy distribution $P(E_T)$ and angular distribution $P(\theta_{CM})$ used to simulate the experimental TOF spectra. The collision energies are 5.0 kcal/mol (a) and 3.5 kcal/mol (b). Here the $P(E_T)$ curves of the two channels are scaled to the same height for visualization.

energies. It should be noted that the separation of ch1 and ch2 is artificial and somewhat arbitrary. Therefore, we fixed the angular distribution of ch2 to be isotropic for simplicity. Figure 4 shows that at both collision energies, ch1 possesses a maximum intensity at $E_T = 2.7$ kcal/mol and $\theta_{CM} = 180°$; ch2 has a very narrow translational energy distribution peaking at 0.2 kcal/mol. This two-channel fitting can well describe the experimental data, indicating that a small fraction of the products with low recoil velocities is less backward than the majority of the product. The $P(E_T)$ and $P(\theta_{CM})$ distributions are very similar for both collision energies, suggesting weak collision energy dependences.

Figure 5 shows a comparison between the experimental and simulated LAB-frame angular distributions of the C_3H_6F product at collision energies of 3.5 and 5.0 kcal/mol. The LAB-frame angular distributions measured at a number of collision energies in the range of 2.3−5.6 kcal/mol all show a very similar shape, indicating the CM-frame angular distributions are also similar in this collision energy range.

No reactive signal can be found if the collision energy is less than 2.0 kcal/mol. To determine the reaction threshold, the excitation function, i.e., the relative reaction cross section as a function of collision energy, was measured. Eight experimental conditions of different collision energies were designed for this purpose. The excitation function is shown in Figure 6 and it was determined by the following procedure: (i) the LAB-frame angular distribution was measured at every collision energy; (ii) the peak height of the angular distribution was normalized with respect to the intensities of both F_2 and C_3H_6 beams; and (iii) then the normalized peak height was plotted as a function of collision energy to give the data in Figure 6. The exhibited excitation function neglects the Jacobian factor in the LAB-to-CM transformation. However, we found that the Jacobian factor varies by less than 15% from collision energies of 3.5 to 5.0 kcal/mol. This factor may affect the shape of the excitation function slightly, but fortunately it will not have a significant influence on the threshold determination. The width of collision energy was deduced from the measured velocity distributions of the molecular beams. The excitation function was fitted with a linear form, $\sigma(E_c) \propto (E_c - E_0)$ for $E_c \geq E_0$, and convoluted with the derived collision energy spread; the collision-energy

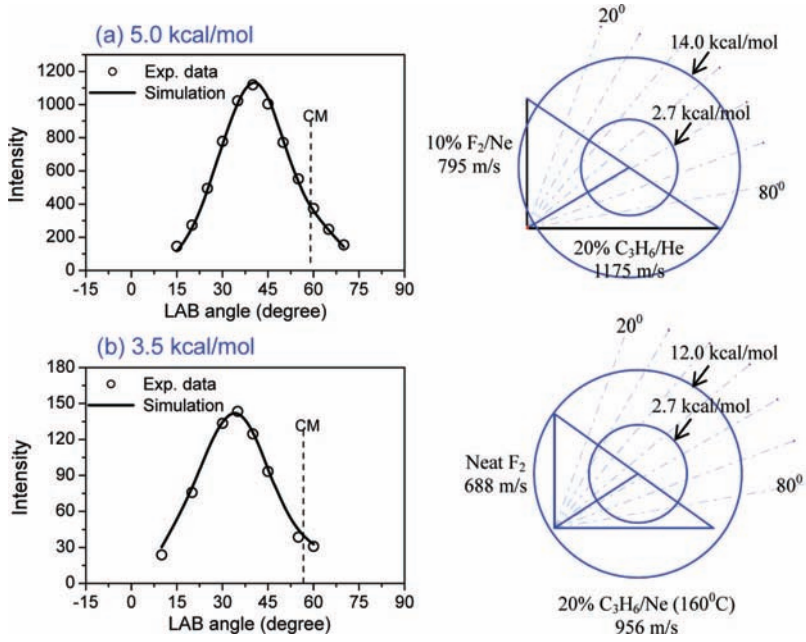

Figure 5. The experimental and simulated LAB-frame angular distributions of the C_3H_6F product. (a) The collision energy is 5.0 kcal/mol; F_2, 795 m/s at 0°; C_3H_6, 1175 m/s at 90°; (b) the collision energy is 3.5 kcal/mol; F_2, 688 m/s at 0°; C_3H_6, 956 m/s at 90°. The corresponding LAB angles of the center of mass are indicated as vertical dashed lines in both panels. The Newton diagram corresponding to each condition is shown nearby.

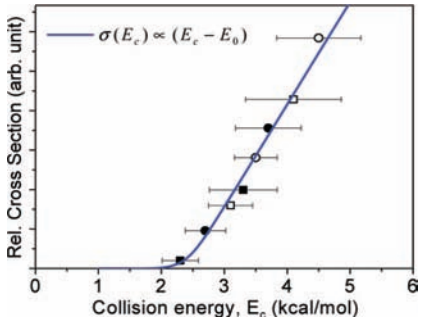

Figure 6. The relative reaction cross section as a function of collision energy. A linear function convoluted with the collision energy spread and fit to the data is shown as a solid line. The threshold energy E_0 is determined to be 2.4 ± 0.3 kcal/mol. The horizontal error bar indicates the width (at half maximum) of the collision energy spread. Different symbols stand for the nozzle temperature used in the experiments: open/closed symbols for the heated/room temperature C_3H_6 nozzle; square/circle symbols for the cryo/room temperature F_2 nozzle (heated = 433 K; room temperature = 300 K; cryo = 150 K).

convolution makes the solid line on Figure 6 a smooth tail around the onset. After considering the collision energy spread, the reaction threshold E_0 was determined to be 2.4 ± 0.3 kcal/mol.

For achieving different beam speeds, various nozzle temperatures were used, which may affect the vibrational excitations of the reactants. In Figure 6, the nozzle temperatures are indicated with different symbols as open/closed symbols for the heated/room temperature C_3H_6 nozzle and square/circle symbols for the cryo/room temperature F_2 nozzle (heated = 433 K; room temperature = 300 K; cryo = 150 K). From these data, we could not find any significant dependence on the nozzle temperature; all data points fall on a smooth line with variations less than experimental uncertainties. This observation indicates that the effect of vibrational excitation in our molecular beams is negligible or its effect is too small to be observed.

To interpret the experimental results, ab initio calculations were performed for reaction R2. The reaction paths and corresponding transition states were searched by the CASPT2 method; the geometries of the reactants and products were optimized with the B3LYP method. Two reaction paths corresponding to F_2 approaching different carbons of the π-bond were found. Similar to the $F_2 + C_2H_4$ reaction, the interaction between the F_2 and C_3H_6 is mainly originated from the coupling between the σ/σ^* orbitals of F_2 and the π/π^* orbitals of C_3H_6, except that the two carbon atoms of the π-bond are no longer symmetric. The optimized transition state structures of these two minimum energy paths are shown in Figure 7 (pathways R2a and R2b). Both transition states have been verified with the intrinsic reaction coordinate (IRC) calculations and vibrational frequency analysis. The vibrational zero-point energies (ZPE) and CCSD(T) electronic energies are summarized in Table 1. The ZPE-corrected complete basis set limit (CBSL) barrier heights for the two transition states TS_1 and TS_2 are 4.4 and 5.2 kcal/mol, respectively. The reaction enthalpies $\Delta H°_{0K}$ of the two reaction pathways R2a and R2b are −8.9 and −9.9 kcal/mol, respectively.

The fraction of translational energy release f_T can be deduced from the formula $f_T = (\langle E_T \rangle)/(E_{avl})$ and summarized in Table 2. For both collision energies, about 30% of the available energy is released into the translational degrees of freedom; the rest (70%) is deposited into the internal degrees of freedom.

We compare the above results with the $F_2 + C_2H_4$ reaction.[5] Dynamics of these two reactions display quite similar features. In both reactions, a fluorine atom plus a fluoro radical was found to be the only observed primary product channel. The HF formation was not observed. The strongly backward-scattered products indicate that the reactions proceed via head-on-like collisions with small impact parameters—a rebound mechanism. In addition, the sharp backward angular distributions imply that the F−F−(π) interactions, pertaining to a C−F bond formation and a F−F bond breaking, approximately lie on a linear line, consistent with the calculated geometries of transition states. According to Polanyi's rule,[21] the transition states in both reactions can be classified as early barriers based on their structures of a higher similarity to the reactants; such dynamics

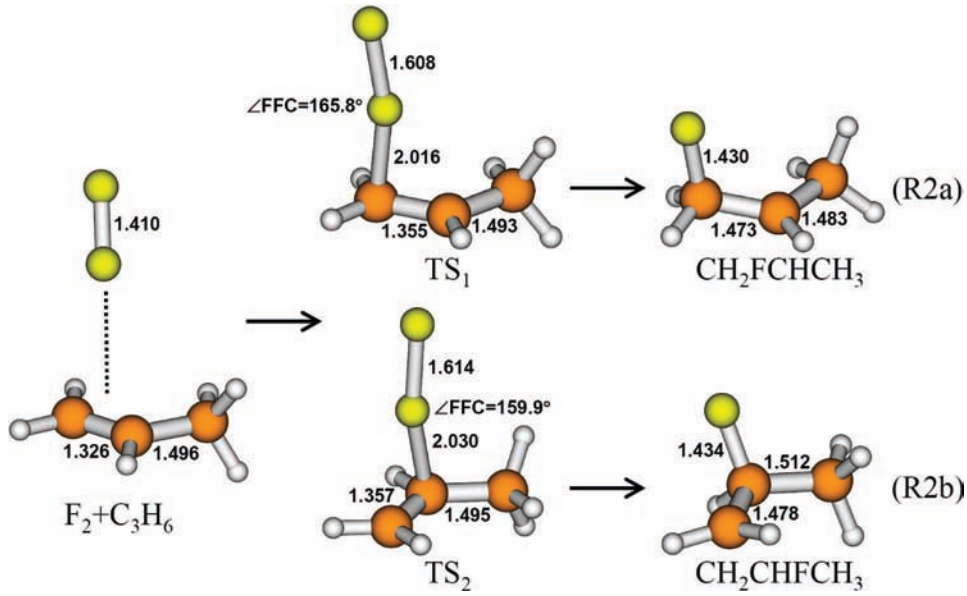

Figure 7. Optimized geometries of F_2, C_3H_6, CH_2FCHCH_3, CH_2CHFCH_3, and two transition states (TS_1 and TS_2). The TS_1 and TS_2 were calculated with the CASPT2 (6e, 6o) method, using the basis sets C = cc-pVTZ, H = cc-pVDZ, and F = aug-cc-pVTZ. The geometries of F_2, C_3H_6, and two products were calculated with the B3LYP method with the same basis sets. Units: Å and deg.

TABLE 1: Vibrational Zero-Point and CCSD(T) Energies

	energy (hartree) for basis sets (N_H, N_C, N_F)[a]				ZPE (hartree)[c]	
	(2,3,3)	(2,4,4)	(2,5,5)	CBSL[b]	B3LYP	CASPT2
F_2	−199.3136	−199.3657	−199.3839	−199.3995	0.00230	0.00212
C_3H_6	−117.6545	−117.6943	−117.7092	−117.7213	0.07933	0.08016
TS_1[e]	−316.9628	−317.0540	−317.0865	−317.1140	0.08230	0.08252
TS_2[e]	−316.9625	−317.0537	−317.0861	−317.1136	0.08246	0.08331
CH_2F-CH-CH_3	−217.3560	−217.4222	−217.4462	−217.4663	0.08127	0.08263
CH_2-CHF-CH_3	−217.3575	−217.4235	−217.4474	−217.4674	0.08081	0.08214
F	−99.6278	−99.6528	−99.6616	−99.6690		

	relative energy (kcal/mol)[d] for basis sets (N_H, N_C, N_F)[a]				ΔZPE (kcal/mol)	
	(2,3,3)	(2,4,4)	(2,5,5)	CBSL[b]	B3LYP	CASPT2
TS_1 barrier	3.47	3.92	4.26	4.41	0.41	0.15
TS_2 barrier	4.14	4.61	5.00	5.18	0.52	0.64
CH_2F-CH-CH_3 $\Delta H°_{0K}$	−9.63	−9.24	−9.05	−8.92	−0.23	0.21
CH_2-CHF-CH_3 $\Delta H°_{0K}$	−10.87	−10.35	−10.08	−9.89	−0.52	−0.10

[a] Notation for the basis sets: H = cc-pVN_HZ; C = cc-pVN_CZ; F = aug-cc-pVN_FZ. [b] CBSL = complete basis set limit. The Hartree−Fock energies were extrapolated with a function of $\exp(-\gamma_1 N)$. The CCSD(T) correlation energies were extrapolated with a function of $\gamma_2 N^{-3}$. [c] ZPE = vibrational zero-point energy calculated with the basis sets of H, C = cc-pVTZ and F = aug-cc-pVTZ. [d] All the relative energies have included ΔZPE_{CASPT2}. [e] TS_1 and TS_2 structures are shown in Figure 7.

TABLE 2: Summary of the Energetic Values for Estimating the Fraction of Translational Energy Release, f_T[a]

reaction pathway	R2a	R2b	R2a	R2b
collision energy	3.5		5.0	
exothermicity	8.9	9.9	8.9	9.9
available energy	12.4	13.4	13.9	14.9
$\langle E_T \rangle$	3.9		4.3	
f_T	0.31	0.29	0.31	0.29

[a] Units: kcal/mol.

is also consistent with the small translational energy release observed for the products.

The calculation shows that F_2 may attack the central and/or the terminal carbon atoms on C_3H_6. However, as can be seen in Table 1, the difference in the barrier heights is only 0.77 kcal/mol, which is too small to determine which one is more favorable. However, an analysis based on the kinematics may help. In the molecular beam experiments, the reactants are rotationally cold such that if F_2 hits the terminal carbon, it will give a larger torque and make the molecule rotate but decrease the interaction between the F_2 and C_3H_6. On the other hand, if F_2 hits the central carbon, it will have a stronger line-of-center force to promote the reaction. Therefore, we believe that the major product channel should be reaction R2b via TS_2, especially when the collision energy is low.

The experimental threshold of 2.4 ± 0.3 kcal/mol is lower than the calculated ones by 2.0 or 2.8 kcal/mol. This situation is quite similar to the F_2 + C_2H_4 reaction, in which the experimental threshold of 5.5 ± 0.5 kcal/mol is lower by 1.6 kcal/mol than the CCSD(T) barrier height of 7.08 kcal/mol. The CCSD(T) calculations seem to overestimate the reaction barrier heights systematically. We may look at this issue in view of the methyl-substitution effect, which lowers the barriers for the F_2 reactions with the π-bonding systems. The experimental value of this barrier lowering is about 3.1 kcal/mol. The calculations also show a significant barrier reduction. Therefore, although there are some overestimations for the CCSD(T) barrier heights,

the calculations show the same trend of the methyl-substitution effect as the experimental observations.

Summary

The dynamics of the $F_2 + C_3H_6$ reaction has been investigated experimentally and computationally. The reaction threshold has been determined to be 2.4 ± 0.3 kcal/mol, which is 3.1 kcal/mol lower than that of the $F_2 + C_2H_4$ reaction. The product distributions show remarkable similarities with the $F_2 + C_2H_4$ reaction. Both experimental and computational results suggest a direct rebound reaction mechanism. Most importantly, the CCSD(T) calculations show a consistent trend of overestimating the reaction thresholds in both $F_2 + C_3H_6$ and $F_2 + C_2H_4$ reactions. For the methyl substitution, both experimental and theoretical results show that methyl substitution efficiently reduces the reaction barrier for the F_2 reaction with small alkenes. Systems with more methyl substituents are under study; further lowering of the reaction barriers can be anticipated. These F_2 + alkene reactions may offer a low-energy route for radical generation without using any catalyst.

Acknowledgment. This work is supported by the National Science Council (grant no. NSC95-2113-M-001-041-MY3) and Academia Sinica, Taiwan.

References and Notes

(1) For example, see: (a) Chambers, R. D. *Fluorine in Organic Chemistry*; Blackwell: Oxford, UK, 2004. (b) Sawaguchi, M.; Hara, S.; Yoneda, N. *J. Fluorine Chem.* **2000**, *105*, 313.

(2) Miller, W. T., Jr.; Dittman, A. L. *J. Am. Chem. Soc.* **1956**, *78*, 2793.

(3) Miller, W. T., Jr.; Koch, S. D., Jr.; McLafferty, F. W. *J. Am. Chem. Soc.* **1956**, *78*, 4992.

(4) Miller, W. T., Jr.; Koch, S. D., Jr. *J. Am. Chem. Soc.* **1957**, *79*, 3084.

(5) Lu, Y.-J.; Xie, T.; Fang, J.-W.; Shao, H.-C.; Lin, J. J. *J. Chem. Phys.* **2008**, *128*, 184302.

(6) Hauge, R. H.; Gransden, S.; Wang, J. L.-F.; Margrave, J. L. *J. Am. Chem. Soc.* **1979**, *101*, 6950.

(7) Frei, H.; Fredin, L.; Pimentel, G. C. *J. Chem. Phys.* **1981**, *74*, 397.

(8) Frei, H.; Pimentel, G. C. *J. Chem. Phys.* **1983**, *78*, 3698.

(9) Frei, H. *J. Chem. Phys.* **1983**, *79*, 748.

(10) Frei, H.; Pimentel, G. C. *Annu. Rev. Phys. Chem.* **1985**, *36*, 491.

(11) Kapralova, G. A.; Chaikin, A. M.; Shilov, A. E. *Kinet. Catal.* **1967**, *8*, 421.

(12) Gyul'bekyan, Z. K.; Sarkisov, O. M.; Vedeneev, V. I. *Kinet. Catal.* **1974**, *15*, 993.

(13) Orkin, V. L.; Chaikin, A. M. *Kinet. Catal. (Engl. Transl.)* **1982**, *23*, 438.

(14) Farrar, J. M.; Lee, Y. T. *J. Chem. Phys.* **1976**, *65*, 1414.

(15) Helgaker, T.; Ruden, T. A.; Jørgensen, P.; Olsen, J.; Klopper, W. *J. Phys. Org. Chem.* **2004**, *17*, 913.

(16) Feller, D.; Peterson, K. A. *J. Chem. Phys.* **2007**, *126*, 114105.

(17) Lin, J. J.; Hwang, D. W.; Harich, S.; Lee, Y. T.; Yang, X. *Rev. Sci. Instrum.* **1998**, *69*, 1642.

(18) Even, U.; Jortner, J.; Noy, D.; Lavie, N. *J. Chem. Phys.* **2000**, *112*, 8068.

(19) Werner H.-J.; Knowles, P. J.; Lindh, R.; Manby, F. R.; Schütz, M., andothers, *MOLPRO*, version 2006.1, a package of ab initio programs; see http://www.molpro.net.

(20) For example, see: (a) Sparks, R. K.; Shobatake, K.; Carlson, L. R.; Lee, Y. T. *J. Chem. Phys.* **1981**, *75*, 3838. (b) Kaiser, R. I.; Ochsenfeld, C.; Stranges, D.; Head-Gordon, M.; Lee, Y. T. *Faraday Discuss.* **1998**, *109*, 183.

(21) Polanyi, J. C. *Acc. Chem. Res.* **1972**, *5*, 161.

JP811053D